Structure of Gum Arabic in Aqueous Solution

YAEL DROR,[1] YACHIN COHEN,[1] RACHEL YERUSHALMI-ROZEN[2,3]

[1]Department of Chemical Engineering, Technion-Israel Institute of Technology, Haifa, Israel 32000, Israel

[2]Department of Chemical Engineering Ben Gurion University of the Negev, Beer Sheva, Israel 84105, Israel

[3]The Ilse Katz Center for Meso- and Nanoscale Science and Technology, Ben Gurion University of the Negev, Beer Sheva, Israel 84105, Israel

Received 30 April 2005; revised 11 July 2006; accepted 22 August 2006
DOI: 10.1002/polb.20970
Published online in Wiley InterScience (www.interscience.wiley.com).

ABSTRACT: Gum arabic, a natural polysaccharide derived from exudates of *Acacia senegal* and *Acacia seyal* trees, is a commonly used food hydrocolloid. The complex chemical structure of the gum has been widely studied revealing a multifraction material consisting mainly of a highly branched polysaccharide and a protein–polysaccharide complex (GAGP) as a minor component. This work investigates its mesoscopic structure in aqueous solution by small-angle X-ray and neutron scattering combined with cryotransmission electrons microscopy. Scattering measurements reveal an intricate shape composed of many spheroidal aggregates assigned to the polysaccharide with a small amount of larger coils. A scattering peak is observed at moderate to high concentrations, the spacing of which exhibits a $c^{-1/3}$ power law relation to polymer concentration (c). Upon addition of salt, this peak disappears, indicating its electrostatic nature. The large coils contribute a q^{-2} power law at the low scattering vector (q) range. However, at low concentration in which the interaggregate peak is not observed, a q^{-1} power law at the low q range indicates the possible existence of a fraction with a locally extended conformation. ©2006 Wiley Periodicals, Inc. J Polym Sci Part B: Polym Phys 44: 3265–3271, 2006

Keywords: gum arabic; hyperbranched; neutron scattering; polysaccharides; SAXS

INTRODUCTION

Gum arabic (GA), a natural composite polysaccharide derived from exudates of *Acacia senegal* and *Acacia seyal* trees, is one of the most commonly used food hydrocolloids. GA serves as a very efficient emulsifier and a long-term stabilizer in food and cosmetic products containing oil–water interfaces. Much research has been conducted over the years to reveal the molecular structure of the gum and to relate it to its exceptional surface-active and rheological properties. It is recognized by many researchers that GA consists of mainly three fractions:[1–4] (1) The major one is a highly branched polysaccharide (MW = 3×10^5) consisting of β-(1→3) galactose backbone with linked branches of arabinose and rhamnose, which terminate in glucuronic acid (found in nature as magnesium, potassium, and calcium salt). (2) A smaller fraction (∼10 wt % of the total) is a higher molecular weight (∼1×10^6 g/mol) arabinogalactan–protein complex (GAGP –GA glycoprotein) in which arabinogalactan chains are covalently linked to a protein chain through serine and hydroxyproline groups. The attached arabinogalactan in the complex contains ∼13% (by mole) glucoronic acid.[5] (3) The smallest fraction (∼1% of the total) having the highest protein content (∼50 wt %) is a glycoprotein which differs in its amino acids composition

Correspondence to: Y. Cohen (E-mail: yachinc@tx.technion.ac.il)

from that of the GAGP complex. Recently, a series of studies on numerous GA samples from a variety of sources was reported, utilizing gel permeation chromatography coupled to multiangle laser light scattering, refractive index, and UV detectors. It showed extensive variation in the molecular weight distributions of the various components between individual samples, even those supplied from a common vendor. Variations are traced to the origin, type, and age of tree, and even to possible effects of processing conditions such as spray dying.[6]

The GAGP complex, although being a minor component, has an important role in both structure and properties of the gum, similar to other hydroxyproline-rich glycoproteins (HRGPs) found in plants. The structure of the complex has not been fully resolved, and two models are currently used for describing the GAGP structure: (1) The "wattle-blossom" model where several arabinogalactan units having molecular weight of $\sim 2 \times 10^5$ g/mol each are described as being attached to a common protein chain forming a compact spheroidal structure.[7] (2) The model used for description of HRGPs such as extensins, arabinogalctan–protein, and others (found in plant cell wall), where a repetitive peptides motif is viewed as composed of a contiguous sequence of hydroxyproline (Hyp) amino acid.[8,9] In the case of GAGP, it was suggested that the protein is built from a "quasi palindrome" sequence. In each side of the serine palindromic center, a block of Hyp residues are attached to short arabinose sequences, while a single noncontiguous Hyp residue is glycosylated with β-(1→3) galactan polysaccharide, according to Hyp-contiguity theory.[5] The chemical nature of these groups results in an extended conformation of the molecule due to the intrinsic rigidity of the Hyp block and the repeating symmetric arrangement of two polysaccharide chains and Hyp-arabinosides.[10] This model is in line with that suggested by Qi et al.,[11] describing the polysaccharide–protein complex as a twisted hairy rope of 150 nm length and 5 nm diameter, in which polysaccharide chains attached in regular intervals are twined around the protein backbone.

It has been suggested that the GAGP complex is apparently the component responsible for the emulsifying and stabilizing properties of the GA, although its specific action and conformation at the interface are not clear yet. The suggestion is based on indications that in oil droplets in emulsions, the adsorbed portion is mainly composed of the high molecular fraction.[1] However, these finding do not exclude the possibility that the adsorption affinity of the polymer is low, and are consistent with the high concentration of GA that is required to achieve full coverage of the oil–water interface and hence effective emulsification and stabilization. The essential role of GAGP in the effectiveness of GA as emulsifier is somewhat contradicted by the observation that arabinogalactan (derived from Larch wood) effectively stabilizes a suspension of metal nanoparticles, exhibiting "protecting agent" performance, that is forming a thick coat around the particle viewed by TEM.[12] Although GA is charged, electrostatic repulsion does not play a dominant role in emulsion stabilization, as indicated by the negative and relatively low value of its ζ-potential (-10 to -20 mV)[13] and by the observation that at the isoelectric point (pH = 1.8) no creaming or flocculation is observed. Thus, the stabilization mechanism is not controlled by electrostatic but rather by steric repulsion. Solutions of GA exhibit low viscosity[14] with shear thinning behavior combined with a Newtonian region at high shear rates as was shown by Mothe and Rao.[15] The low viscosity is attributed to the highly branched structure inducing a relative compact shape.

Recently, the use of GA has been extended to stabilization of solids dispersions, re-exploiting its surface-active properties first discovered by the ancients. It was found that GA may act as a stabilizer for oxide dispersions as well as a bridging agent forming a strong network depending on the type of oxide and pH condition.[16] A new approach has achieved good results in dispersing individual carbon nanotubes in aqueous solution by GA.[17] GA dispersions exhibited a homogenous black appearance similar to the ink produced by the ancient Pharaohs with GA and carbon black. Interestingly, arabinogalactan did not stabilize single-walled carbon nanotubes in aqueous solutions, unlike GA.[18]

Despite the remarkably wide use of GA over many years and intense research concerning its chemical structure, it seems that very little is known about its mesoscopic structure in water and at the interface in dispersions. The main purpose of this work is to characterize the microstructure of GA in aqueous solution using scattering methods that enable the evaluation of the overall structure as well as the inner heterogeneity. This is combined with direct microscopic imaging. The structural information may be used to improve our understanding of the special physical properties of GA.

EXPERIMENTAL

Materials and Solution Preparation

Solutions of GA (Aldrich, *Acacia* 26,077-0) were prepared using Millipore water (resistance of 18.2 MΩ cm) at different concentrations at room temperature. The solutions were gently hand shaken until homogenous transparent mixtures were achieved. For small-angle neutron scattering (SANS) measurements, GA was dissolved in D_2O (Sigma–Aldrich). Solutions at the same concentrations of natural arabinogalactan from Larch wood (Sigma–Aldrich) were prepared in the same way.

Small-angle X-ray scattering (SAXS) measurements were performed with Cu Kα radiation (Ni-filtered) using a compact Kratky camera with a linear position sensitive detector. The collimating slit dimensions defining the line-shaped beam were 20 μm in width and 15 mm in length. The sample solutions were placed in a quartz cylindrical cell of 0.92 mm diameter. The measurements were done at a controlled temperature of 25 °C. The primary beam intensity was determined by the moving-slit method and the measurement of a thin quartz monitor used as a secondary standard. The measured intensity was corrected for sample absorption, measured independently. Finally, the measured data were corrected for the "smearing" effect arising from the slit-collimated incident beam. For solution concentrations of 0.5% and higher, which exhibit a scattering peak due to partial order, de-smearing was performed using the indirect transformation in reciprocal space procedure (ITR).[19] For solution concentrations of 0.5% and lower de-smearing was also performed using the indirect Fourier transformation procedure (ITP).[20] The data are presented as intensity (at absolute units) as a function of the scattering vector ($q = 4\pi \sin\theta/\lambda$ where 2θ is the scattering angle and λ is the wavelength).

SANS measurements were carried out at the KWS1 diffractometer at the FRJ-2 research reactor in Fz-Jülich, Germany, and on the LOQ beamline at the ISIS facility (DRAL, UK). The samples were filled in 2 mm path length quartz cells. At KWS1, the incident wavelength was 0.7 nm and the sample aperture was 10 × 10 mm^2. These measurements were performed at three detector/collimation distances to cover a wide range of scattering vectors from ~0.02 to 2.0 nm^{-1}. At LOQ, the incident wavelength was 0.2 nm and the accessible scattering vectors ranged from 0.07 to 2.8 nm^{-1}. The raw data were corrected for the empty cell, detector efficiency, and background scattering. The absolute intensity (cm^{-1}) was obtained using secondary scattering standards.

Cryotransmission Electron Microscopy

Vitrified samples of GA were prepared in a controlled environment vitrification system (CEVS)[21] at a controlled temperature of 25 °C and 100% relative humidity. The transfer of the sample to the microscope was done using an Oxford Instruments CT-3500 cryospecimen holder and transfer system. The samples were investigated using low electron dose imaging and acceleration voltage of 120 kV in a Philips CM120 TEM. Images were recorded with a Gatan MultiScan 791 CCD camera, using the Gatan DigitalMicrograph 3.1 software package.

RESULTS AND DISCUSSION

The overall structure of GA was studied by X-ray and neutron scattering at different concentrations at room temperature. X-ray scattering patterns of GA at different concentrations are shown in Figure 1. It can be clearly seen that the scattering pattern is characterized by a well-defined peak. The measured data were corrected for the dimensions of the incident slit-collimated beam ("de-smearing") using the indirect

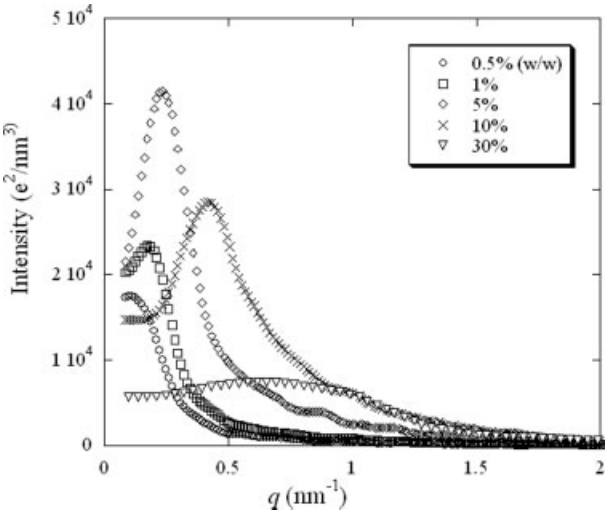

Figure 1. SAXS patterns of GA solutions at different concentrations.

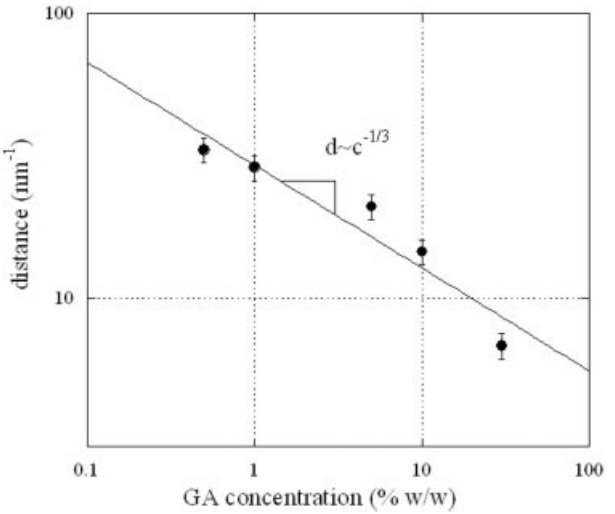

Figure 2. Interaggregate spacing, d, at different concentrations of GA solutions as calculated from the maximum peak position measured by SAXS.

transformation in reciprocal space procedure (ITR), which is suited for partially ordered systems which exhibit scattering maxima.[19] The position, shape, and intensity of the peak depend on the concentration of the solution. As the concentration increases, the peak shifts to higher values of the scattering vector, and broadens. This kind of scattering behavior characterizes assemblies of scattering moieties ("aggregates") with interaggregate correlations. As the concentration increases, the distance between aggregates decreases, due to crowding of the aggregates. This behavior is qualitatively different from intraparticle effects, where changes in the scattering pattern result from changes in the shape (form factor) of the individual aggregate, and are thus unaltered by the concentration. At the highest measured concentration (30% w/w), the peak becomes significantly broader due, we believe, to the onset of overlap of polymer aggregates. Interestingly, viscosity measurements show a sharp increase at about the same concentration,[15,22] as expected at overlap concentration of the polymer (c^*).[23] The high overlap concentration, unusual for linear polymers of comparable molecular weight, is in accordance with the view of the major component of GA as a hyperbranched polymer forming an overall spheroidal shape with negligible intermolecular contact up to high concentration.

The periodicity spacing of GA aggregates (d, nm) in solutions as a function of concentration was determined from the peak position (q^*) by Bragg's law ($d = 2\pi/q^*$) and is shown in Figure 2. The results clearly follow a $q^{-1/3}$ power law, unlike common polyelectrolyte solutions at comparable concentrations, which exhibit a $q^{-1/2}$ dependence.[24] The $-1/3$ power is typical to a packing of spherical aggregates or dilute polyelectrolyte solutions.[25] A similar power-law relation of peak position with concentration was observed in SANS patterns from charged polymer dendrimers in water.[26] This result is consistent with that of the highly branched and compact nature of the polysaccharide GA. Interestingly, the Bragg spacing estimated at the overlap concentration, on the order of 10 nm, is about twice the radius of gyration evaluated for the polysaccharide in the main fraction of GA.[27]

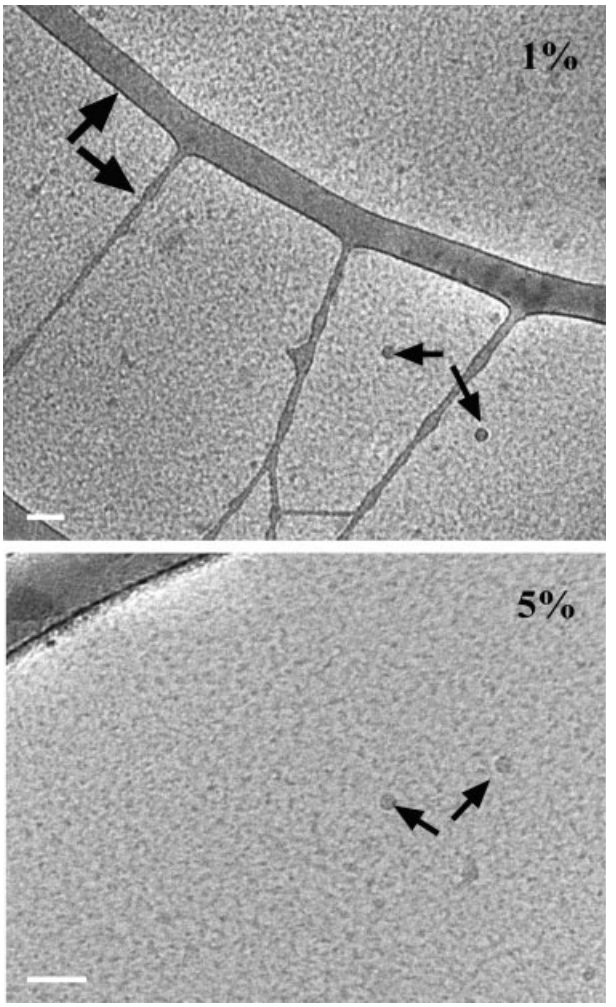

Figure 3. Cryo-TEM micrographs of aqueous solutions of GA at concentrations of 1% (top) and 5% w/w (bottom). Thin arrows indicate larger aggregates or possible ice spots and thick arrows point at the holey carbon film. Bar = 50 nm.

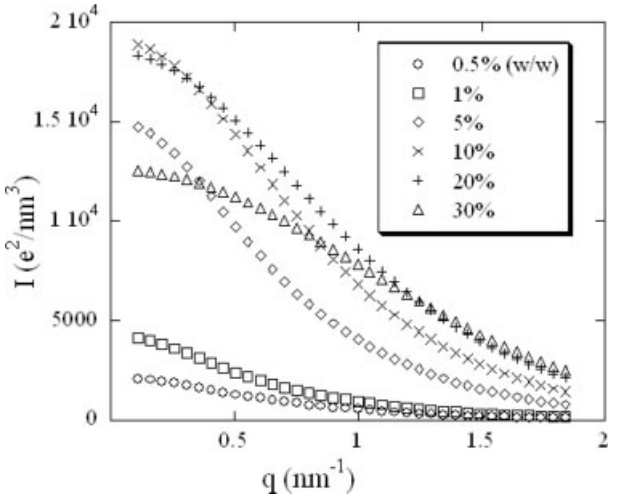

Figure 4. SAXS curves of aqueous solutions of arabinogalactan at different concentrations.

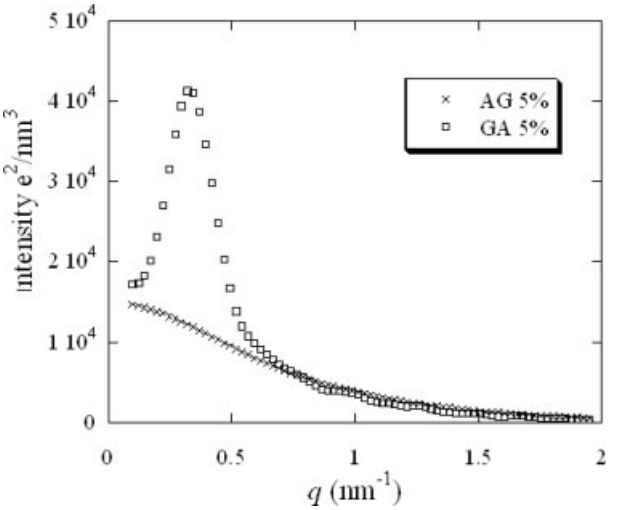

Figure 5. SAXS curves of aqueous solutions of GA (□) and AG (×) at a concentration of 5% (w/w).

Cryo-TEM micrographs of aqueous solutions of GA (1% (top) and 5% w/w (bottom)) are presented in Figure 3. The predominant features are compact spheroidal structures, which may be attributed to the major polymer component of GA, the diameter of which appears to be less than 10 nm. Some occurrence of larger spheroidal structures may be noticed, as indicated by thin arrows in Figure 3. These may be due to the larger components of GA, or possibly to sporadic ice nuclei in the vitrified dispersion.

To probe the origin of the structure revealed by the scattering patterns presented earlier, we investigated the scattering from aqueous solutions of arabinogalactan (AG, extracted from Larch tree) at similar concentrations. As clearly observed in Figure 4, the scattering patterns of these solutions differ significantly from those exhibited by GA at similar concentrations. In particular, while the scattering patterns of GA solutions are dominated by a clear peak, no such peak is observed at any concentration of AG. In Figure 5, we present a superposition of the scattering patterns of aqueous solutions of GA and aqueous solutions of arabinogalactan at a concentration of 5% (w/w). The pronounced difference between the two scattering curves suggests that the solution behavior of the two biopolymers is very different, as indeed observed. It is also interesting to note that as in case of the GA, a pronounced decrease in the intensity is observed at 30% (w/w) AG concentration, due to intermolecular correlations.

The structure of GA solutions at different salt concentrations was measured by SANS. Added salt does not affect significantly the background level of the SANS pattern, as compared to SAXS, since in the former it is mainly due to incoherent scattering from the polymer's hydrogen nuclei. We observed that as the salt concentration increases, the peak gradually disappears (Fig. 6). This result indicates that an electrostatic interaction determines the distance between the GA aggregates, as is the case in simple polyelectrolytes[25] and charged polymer dendrimers.[26] Once the electrostatic interaction is screened by the salt, the electrostatic barrier is removed and the peak disappears. Recent scattering study on Whey protein/GA coacervates

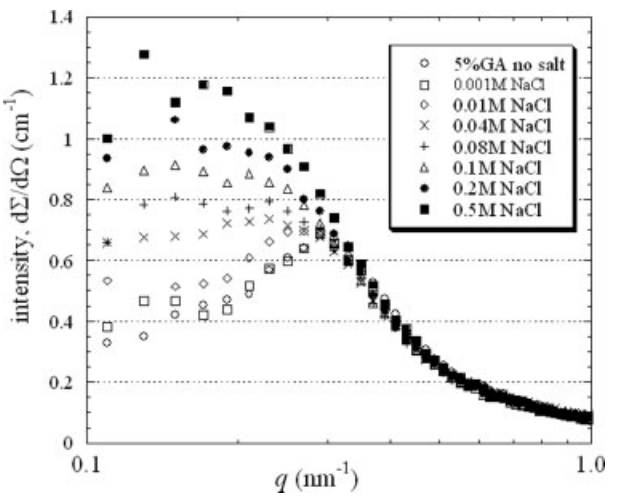

Figure 6. SANS patterns of 5% GA in D_2O with different concentrations of NaCl, after subtraction of background scattering from the salt solution.

exhibited a similar effect. Since the complexion between these two components is based on electrostatic interaction (between oppositely charged entities), the masking of the charged groups of GA by the addition of salt directly affected the structure of the coacervates.[28] The absence of the electrostatic peak in arabinogalactan may be attributed to the fact that the arabinogalactan consists of only a small amount of acidic groups (~0.2%) compared with GA.[12,22]

The X-ray scattering patterns of GA at concentrations below 0.4%(w/w), shown in Figure 7, reveal a new feature that is not observed at higher concentrations: excess scattered intensity in the small q range ($q < 0.15$ nm^{-1}), which tends to scale with the scattering vector to a power nearly -1. It should be noted that the scattering from these dilute solutions was evaluated using the indirect transform ITP,[20] which is suitable for isolated scattering objects with no long range order. The difference in the scattering patterns may be an indication for stiff-chain behavior in the dilute solutions.[29] This phenomenon may be attributed to the protein chain of the higher molecular weight GAGP complex, which may acquire locally a more extended conformation at low concentrations (and lower ionic strength). At low concentrations, the protein complex may locally attain an extended conformation, while at higher concentrations, the chain is more contracted. This phenomenon was not observed in arabinogalactan solutions, suggesting

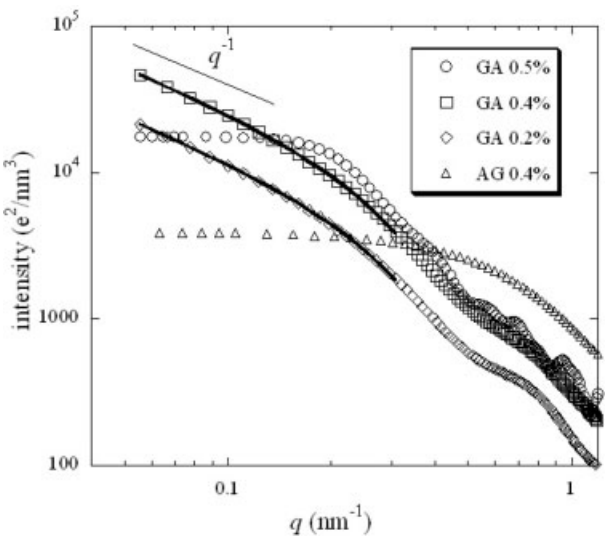

Figure 7. SAXS patterns of aqueous solutions of GA and AG at low concentrations. The solid lines are fits of the measured data according to eq 1.

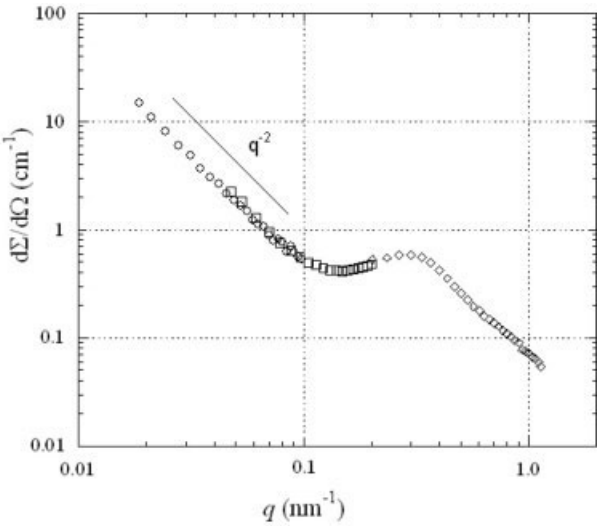

Figure 8. SANS pattern of 5% (w/w) GA at three detector/collimation distances: 20 m (circles), 8 m (squares), and 2 m (diamonds).

that indeed the presence of the GAGP complex may be involved. The scattering pattern at this low q range was fit to a rod-like particle model, where the length is much larger than the diameter, according to the Guinier approximation:[29]

$$I = \frac{A}{q}\exp\left(-\frac{R_c^2 q^2}{2}\right) \quad (1)$$

where A is a prefactor and R_c is the radius of gyration of the cross section. The fit of eq 1 to the measurements, shown in Figure 7, yields a value of 4 ± 0.03 nm for the gyration radius of the cross section. This is in reasonable agreement with the elongated structure model proposed by Qi et al.[11]

At a higher concentration (5% w/w), the SANS pattern measured at the lowest accessible q range (0.02–0.1 nm^{-1}) reveals a pronounced intensity increase at small q, which seems to follow a q^{-2} power-law (Fig. 8). This may be an indication for a Gaussian chain like behavior following the Debye function:[30]

$$I(q) = \frac{e^{(-q^2R_g^2)} - 1 + q^2R_g^2}{q^4R_g^4} \quad (2)$$

Since the -2 power law appears at small scattering vectors, the radius of gyration of the coil must be significantly large (tens of nanometers, as $q\ R_g \gg 1$). Indeed, a large hydrodynamic radius (R_h) of the fractionated GAGP was reported by Islam et al. (22.9 nm).[3]

CONCLUSIONS

X-ray and neutron scattering measurements shed light on the overall shape of gum arabic, as composed of many spheroidal structures of the major component, that is a hyperbranched charged polysaccharide, interlaced with a small amount of large coils of GAGP. The high molecular weight of GAGP combined with the fact that the protein backbone is glycosylated with charged branched arabinogalactan side chains, which inhibit a compact conformation, can indeed rationalize such a large coil. Thus the scattering pattern represents the sum of these two populations. There is some indication for the appearance of a locally extended structure at very low concentrations, which may be due to the GAGP complex. The next step toward full evaluation of the complex structure of GA requires scattering analysis of the isolated fractions of the gum. Then the fine structure describing the shape of the protein core and the attached polysaccharides in the GAGP, as well as the shape of the unbounded polysaccharide may be better evaluated.

The authors acknowledge the support of the Israel Science Foundation [grant no. 287/00 (Y. Cohen), and Center of excellence program, grant no. 8003(R. Yerushalmi-Rozen)]. For the SANS measurements at ISIS, we thank R. K. Heenan and acknowledge support from the European Community—Access to Research Infrastructure. For the SANS measurements at Fz. Jülich we thank W. Pyckhout-Hintzen and acknowledge support by the Jülich Neutrons for Europe program.

REFERENCES AND NOTES

1. Randall, R. C.; Phillips, G. O.; Williams, P. A. Food Hydrocolloids 1988, 2, 131.
2. Fenyo, J. C.; Vandervelde, M. C. In Gum and Stabilizer for the Food Industry; IRL Press: Oxford, 1990; Vol. 5, pp 17–23.
3. Islam, A. M.; Phillips, G. O.; Sljivo, A.; Snowden, M. J.; Williams, P. A. Food Hydrocolloids 1997, 11, 493.
4. Idris, O. H. M.; Williams, P. A.; Phillips, G. O. Food Hydrocolloids 1998, 12, 379.
5. Goodrum, L. J.; Patel, A.; Leykam, J. F.; Kieliszewski, M. J. Phytochemistry 2000, 54, 99.
6. (a) Al-Assaf, S.; Phillips, G. O.; Williams, P. A. Food Hydrocolloids 2005, 19, 647; (b) Al-Assaf, S.; Phillips, G. O.; Williams, P. A. Food Hydrocolloids 2005, 19, 661; (c) Hassan, E. A.; Al-Assaf, S.; Phillips, G. O.; Williams, P. A. Food Hydrocolloids 2005, 19, 669; (d) Siddig, N. E.; Osman, M. E.; Al-Assaf, S.; Phillips, G. O.; Williams, P. A. Food Hydrocolloids 2005, 19, 679; (e) Flindt, C.; Al-Assaf, S.; Phillips, G. O.; Williams, P. A. Food Hydrocolloids 2005, 19, 687.
7. Connolly, S.; Fenyo, J. C.; Vandervelde, M. C. Carbohydr Polym 1988, 8, 23.
8. Kieliszewski, M. J.; Lamport, T. A. Plant J 1994, 52, 157.
9. Gaspar, Y.; Johnson, K. L.; McKenna, J. A.; Bacic, A.; Schultz, C. J. Plant Mol Biol 2001, 47, 161.
10. Lodish, H.; et al. In Molecular Cell Biology; Scientific American Books Inc.: New York, 1995; Ch. 24.
11. Qi, W.; Fong, C.; Lamport, D. T. A. Plant Physiol 1991, 96, 848.
12. Mucalo, M. R.; Bullen, C. R.; Manley-Harris, M.; McIntire, T. M. J Mater Sci 2002, 37, 493.
13. Jayme, M. L.; Dunstan, D. E.; Gee, M. L. Food Hydrocolloids 1999, 13, 459.
14. Huang, X.; Kakuda, Y.; Cui, W. Food Hydrocolloids 2001, 15, 533.
15. Mothe, C. G.; Rao, M. A. Food Hydrocolloids 1999, 13, 501.
16. Leong, Y. K.; Seah, U.; Chu, S. Y.; Ong, B. C. Colloids Surf A 2001, 182, 263.
17. Bandyopadhyaya, R.; Nativ-Roth, E.; Regev, O.; Yerushalmi-Rozen, R. Nano Lett 2001, 1.
18. Nativ-Roth, E.M.Sc. Thesis, Ben-Gurion University, Beer Sheva, Israel, 2004.
19. Glatter, O.; Gruber, K. J Appl Crystallogr 1993, 26, 512.
20. Glatter, O. J Appl Crystallogr 1977, 10, 415.
21. Bellare, J. R.; Davis, H. T.; Scriven, L. E.; Talmon, Y. J Electron Microsc Tech 1988, 10, 87.
22. Whistler, R. L.; BeMiller, J. N. Industrial Gums: Polysaccharides and Their Derivatives; Academic Press: London, 1973.
23. de Gennes, P. G. Scaling Concepts in Polymer Physics; Cornell University Press: Ithaca, 1979; p 76.
24. de Gennes P. G.; Pincus, P.; Velasco, R. M.; Brochard, F. J Phys (Paris) 1976, 37, 1461.
25. Nishida, K.; Kaji, K.; Kanaya, T.; Shibano, T. Macromolecules 2002, 35, 4084.
26. Nisato, V.; Ivkov, R.; Amis, E. J. Macromolecules 1999, 32, 5895.
27. Picton, L.; Bataille, I.; Muller, G. Carbohydr Polym 2000, 42, 23.
28. Weinbreck, F.; Tromp, R. H.; Kruif, C. G. Biomacromolecules 2004, 5, 1437.
29. Glatter, O.; Kratky, O. Small Angle X-Ray Scattering;Academic Press: London, 1982; p 34.
30. Roe, R. J. Methods of X-Ray and Neutron Scattering in Polymer Science; Oxford University Press: New York, 2004; p 164.